

Galaxy Evolution in the Reddest Possible Filter

E. A. Richards (erichard@nrao.edu)

National Radio Astronomy Observatory & University of Virginia, 520 Edgemont Road, Charlottesville, VA 22903, USA

Abstract.

We describe an observational program aimed at understanding the radio emission from distant, rapidly evolving galaxy populations. These observations were carried out at 1.4 and 8.5 GHz with the VLA centered on the Hubble Deep Field, obtaining limiting flux densities of 40 and 8 μ Jy respectively. The differential count of the radio sources is marginally sub-Euclidean to the completeness limits ($\gamma = -2.4 \pm 0.1$) and fluctuation analysis suggests nearly 60 sources per arcmin² at the 1 μ Jy level. Using high resolution 1.4 GHz observations obtained with MERLIN, we resolve all radio sources detected in the VLA complete sample and measure a median angular size for the microjansky radio population of 1-2''. This clue coupled with the steep spectral index of the 1.4 GHz selected sample suggests diffuse synchrotron radiation in $z \sim 1$ galactic disks.

The wide-field HST and ground-based optical exposures show that the radio sources are identified primarily with disk systems composed of irregulars, peculiars, interacting/merging galaxies, and a few isolated field spirals. Only 20% of the radio sources can be attributed to AGN – the majority are likely associated with starburst activity. The available redshifts range from 0.1-3, with a mean of about 0.8. We are likely witnessing a major episode of starburst activity in these luminous ($L > L^*$) systems, occasionally accompanied by an embedded AGN.

About 20% of the radio sources remain unidentified to $I = 26-28$ in the HDF and flanking fields. Several of these objects have extremely red counterparts. We suggest that these are high redshift dusty protogalaxies.

1. A Radio Perspective of Galaxies

Determining how galaxies form and subsequently evolve remains a subject of intense study despite decades of research. Traditionally, astronomers primarily have used optical methods to study the characteristics of local and distant galaxies. With the discovery of the infra-red ultraluminous galaxies in the early 1980s (e.g., Soifer et al. 1984), it was soon recognized that optical studies can severely bias the understanding of galaxy properties due to dust obscuration, especially in those systems undergoing enhanced episodes of star-formation activity (i.e., a starburst galaxy).

The far infrared (FIR) radiation ($30 \mu\text{m} < \lambda < 300 \mu\text{m}$) of a starburst is composed of reprocessed ultraviolet(UV) and optical light from young, recently formed stellar populations. This radiation is absorbed by dust in the interstellar medium and thermally reradiated at FIR



wavelengths. Closely related to the FIR emission in starburst galaxies is the radio continuum. Although the radio emission is linked to active star-formation by different physical mechanisms than that of the FIR, there is a tight correlation between the FIR and radio luminosity of a starburst (Helou et al. 1985).

In normal galaxies (i.e., without a powerful AGN), the centimeter radio luminosity is dominated by diffuse synchrotron emission believed to be produced by relativistic electrons accelerated in supernovae remnants. Detailed radio studies of nearby starburst galaxies such as M82 (Kronberg et al. 1985, Muxlow et al. 1994) and Arp 220 (Smith et al. 1998) have revealed large numbers of young radio supernovae, embedded in extended synchrotron haloes formed by a combination of old, coalesced SNRs and cosmic ray injection into the surrounding disks of these galaxies. As the synchrotron radiation of a starburst dissipates on a physical time scale of $10^7 - 10^8$ years, the radio luminosity is a true measure of the *instantaneous* SFR in a galaxy, uncontaminated by older stellar populations. Furthermore, since supernovae progenitors are dominated by $\sim 8 M_\odot$ stars, synchrotron radiation has the additional advantage of being less sensitive to uncertainties in the initial mass function as opposed to UV and optical recombination line studies. Because galaxies and the inter-galactic medium are transparent at centimeter wavelengths, radio emission is a sensitive measure of star-formation in distant galaxies.

Comparison of the local radio luminosity function (LF) of star-forming galaxies (Condon 1989) with those derived independently at FIR (Soifer et al. 1987), H α (Gallego et al. 1995), and UV wavelengths (Treyer et al. 1998) shows good agreement (Cram 1998). Figure 1 shows the four LFs in units of SFRs. This analysis suggests the bulk of local star formation is occurring in modest starbursts with $\text{SFR} \sim 10 M_\odot \text{ yr}^{-1}$. However, past the peak in the LF, the H α and UV estimates begin to fall below the radio/FIR rates, and at about $50 M_\odot \text{ yr}^{-1}$ has entirely vanished. The radio source counts and redshift statistics are both consistent with pure luminosity evolution of the local population to $z \sim 1$ with $L \propto (1+z)^{3.5}$ (e.g., Rowan-Robinson et al. 1993). Thus the peak in the star-forming RLF at $z \sim 1$ likely moves past a few hundred $M_\odot \text{ yr}^{-1}$ where optically selected surveys become severely biased. Deep radio surveys, sensitive to star-forming galaxies to $z \sim 2$, provide unique information on distant, rapidly evolving galaxy populations.

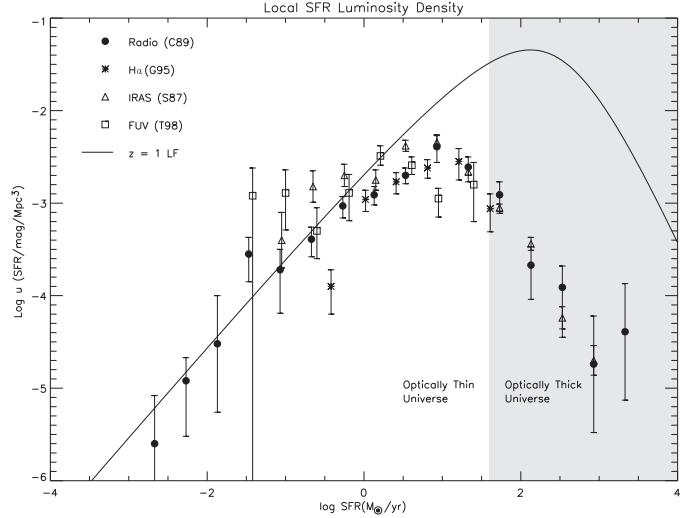


Figure 1. Shown is the contribution to the local star-formation luminosity density (u) per luminosity interval of star-forming galaxy. The radio, IRAS, $H\alpha$, and far-ultraviolet (FUV) luminosity functions have been converted to SFRs assuming a Salpeter IMF over $0.1\text{--}100 M_\odot$. The shaded region represents what may be a dust curtain beyond which optical surveys are blind to star formation. If the SFR luminosity function evolves as $L \propto (1+z)^{3.5}$, then by $z=1$, it will appear as the solid line. This analysis suggests that the bulk of global star-formation at high- z is hidden from optical surveys.

2. Radio Observations of the Hubble Deep Field

The HDF has been observed previously with the VLA at 8.5 GHz to a one sigma sensitivity of $1.8 \mu\text{Jy}$ (Richards et al. 1998). In June 1997 we observed the HDF region for an additional 40 hours at 8.5 GHz. We mosaiced an area defined by four separate pointings offset from the center of the HDF by the half-power point of the primary beam response ($2.7'$) in the cardinal directions for about 10 hours duration each. The final combined 8.5 GHz images have an effective resolution of $3.5''$ and a completeness limit of $8 \mu\text{Jy}$ which rises to $40 \mu\text{Jy}$ at $6.6'$ from the HDF center. Within this area we detected 40 sources in a complete (5σ) with an additional 19 sources in a supplementary sample ($3.5\text{--}5 \sigma$).

In November 1996, we observed the HDF at 1.4 GHz with the VLA. The observational details and data processing are discussed by Richards (1999). The 1.4 GHz VLA image covers $40'$ diameter with an effective resolution of $1.8''$ and an rms noise of $7.5 \mu\text{Jy}$. We defined a complete-

The Angular Size Distribution of the Radio Sources in the HDF and HFF

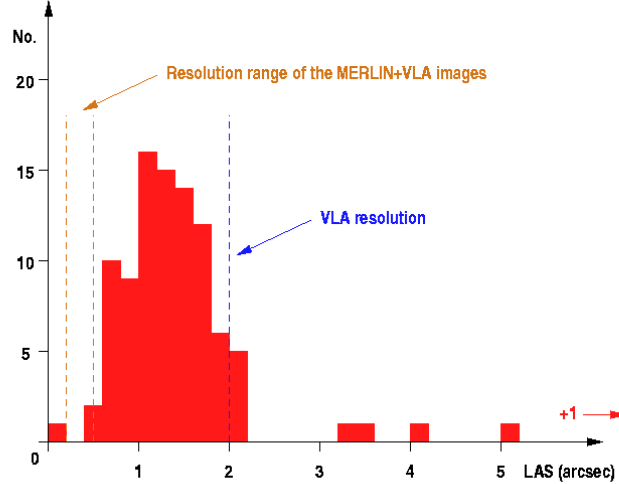


Figure 2. Angular sizes of sources detected in the VLA+MERLIN images.

ness limit of $40\mu\text{Jy}$ to compose a catalog of 371 radio sources of which 30 were detected at 8.5 GHz. In total 16 radio sources lie in the HDF.

In February 1996 and April 1997, we observed the HDF with the MERLIN interferometer at 1.4 GHz for a total of 17×24 hours. These data were combined with the VLA data to produce sky images around all 89 previously known radio sources in the inner $10' \times 10'$ of the field. These high resolution 1.4 GHz images have a rms noise of $3.3 \mu\text{Jy}$ at $0.2''$ resolution (Muxlow et al. 1999).

3. Radio Angular Sizes and Spectra

All previous high resolution studies of submillijansky radio sources have been limited to approximately $2''$ resolution. Because the median angular size is known to change rather sharply below a few millijansky at 1.4 GHz (presumably due to the emergence of a new population) from $\sim 10''$ to a few arcsec, our present observations are uniquely suited to study the radio morphologies of the faintest radio sources for the first time.

Figure 2 shows the angular sizes of the 89 sources detected by both MERLIN and the VLA. Virtually all radio sources are resolved at $0.2''$ resolution. There are very few radio sources with sizes greater than a few arcsec which are generally associated with classical FR I and

II radio galaxies. Rather, the median angular size for our sample is between $1\text{-}2''$, indicative of radio emission on galactic or sub-galactic scales.

The spectral index ($S \propto \nu^{-\alpha}$) of a source can be used to diagnose the origin of the radio emission. Inverted spectrum sources are invariably associated with self-absorbed synchrotron emission associated with an AGN. Flat spectrum sources ($0 < \alpha < 0.5$) can be produced by AGN or optically thin Bremsstrahlung radiation from star-formation at higher ($\nu > 5$ GHz) radio frequencies. Steep spectrum sources ($\alpha > 0.5$) consist of diffuse synchrotron emission, often associated either with radio jets or star-formation in galaxies.

For the 8.5 GHz selected sample in the HDF, the median spectral index is $\alpha_{8.5} = 0.35$. Less than 15% of these sources are inverted. Although several of these radio sources are dominated by an AGN, many show diffuse radio emission which is likely a combination of diffuse synchrotron and free-free radiation associated with wide-scale star formation. The 1.4 GHz selected sample has a median spectral index $\alpha_{1.4} = 0.85$. Thus the microjanksy radio population at 1.4 GHz is dominated by sources with diffuse synchrotron emission.

4. Optical Identifications

The absolute astrometric accuracy of our interferometric images is set by our phase calibrator which has a position error of $0.02''$. The independent VLA and MERLIN radio positions for sources detected in the HDF agree to $0.04''$. The HDF WFPC2 images were previously aligned to the radio reference frame to about $0.1''$ accuracy (Williams et al. 1996). We bootstrapped each of the eight individual WFPC2 flanking field images to the radio grid by first aligning a widefield I-band image provided to us by Barger et al. (1999) with our radio sources. Optically bright galaxies detected in both the HST and the ground-based images were used to register the individual WFPC2 frames to an accuracy of $0.1\text{-}0.2''$.

Of the 91 radio sources contained in published optical images (Barger et al. 1999), 72 have clear identifications with reliabilities ranging from 95-99% (Richards et al. 1998). Figure 3 presents the magnitude histogram of these galaxies. The mean of the identifications is $I = 22$ mag, with a clear decline in the distribution past $I = 23$ mag. Sixteen radio sources cannot be identified in the HFFs or ground-based images, and three fields are blank in the HDF itself.

Of the radio sources identified, the majority reside in disk systems composed of mergers, irregulars, and/or isolated spiral galaxies

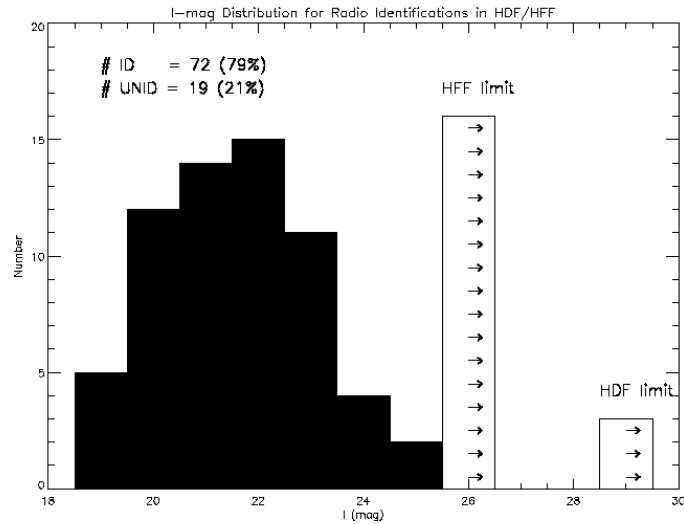


Figure 3. I magnitude histogram of radio sources in the HDF region.

(Richards et al. 1998). A few red ellipticals are apparent which are almost certainly AGN. Of the radio sources with redshifts, most are at $z = 0.4$ -1 but we caution that there still exists 70% incompleteness in the sample. Many of the disk systems identified as radio sources have clear indications of active star-formation, including prominent but narrow emission lines ([OII] and H α), mid-infrared excesses (Aussel et al. 1999) or peculiar optical morphology. These clues coupled with the diffuse, steep spectrum radio emission give strong evidence that the *majority of radio sources in the HDF region are starburst galaxies*. The implied starformation rates for those galaxies with redshifts range from $10 M_{\odot}$ /yr to 1000s M_{\odot} /yr. Two of the radio starbursts we typically detect are shown in Figure 4.

4.1. CANDIDATE HIGH- z RADIO SOURCES

Although the majority of radio sources in the HDF region can be identified with rather bright optical galaxies ($I \sim 22$ mag.), 20% of the sources remain in blank fields. These sources range in significance from 6 - 100 σ . Deep infrared imaging exists for several of these radio sources (Barger et al. 1999, Waddington et al. 1999) which shows some fraction to have very red colors consistent with them being high redshift

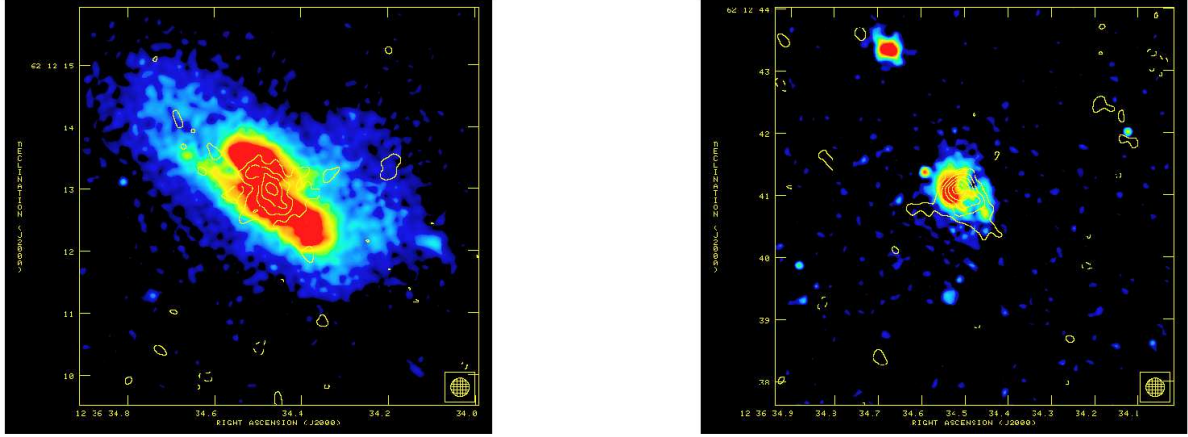


Figure 4. Left) Radio contours for VLA J123634+621212 are overlaid on the WFPC2 image of this $I = 19$ mag. merging system at $z = 0.46$ (Cohen et al. 1996). This radio source also has a firm ISO detection (Aussel et al. 1999). The radio SFR = $140 M_{\odot} / \text{yr}$. The radio emission peak is coincident with a prominent dust lane. Right) VLA J123634+621240 is another candidate merger at $z = 1.22$ (Cohen 96) and with a bright ISO detection (Aussel et al. 1999). The steep spectrum radio emission implies a SFR = $2100 M_{\odot} / \text{yr}$.

galaxies ($z > 2$). Figure 5 shows two such optically unidentified radio objects.

Recently, the HDF has been imaged to the confusion limit by the JCMT/SCUBA at $850 \mu\text{m}$ (Hughes et al. 1998). Intriguingly, two of the radio sources unidentified in the HDF lie within a few arcsec of the brightest two sub-mm sources. This is especially significant given that the SCUBA beam is $15''$ in diameter. VLA J123651+621221 is a steep spectrum radio source contained in both the complete 1.4 and 8.5 GHz samples and is partially resolved by the $0.2''$ MERLIN beam. Dickinson (private communication) reports a very red object at the position of the radio source giving further evidence to its unusual nature.

In Cycle 7, we obtained NICMOS imaging of our brightest unidentified radio object (VLA J123642+621331) in J and H filters (Waddington et al. 1999). We obtained a firm detection in H, yielding a color of $I - H > 3.3$. Surprisingly, the light profile of the underlying galaxy is exponential with a half-light radius of $0.13''$. This is strongly suggestive of a nuclear starburst galaxy at substantial redshift.

What are these unidentified radio objects? We consider four possibilities:

1. moderate z ellipticals - Red ellipticals ($I - K > 4$) at redshifts 1-2 are not uncommon. However, the radio sources under discussion

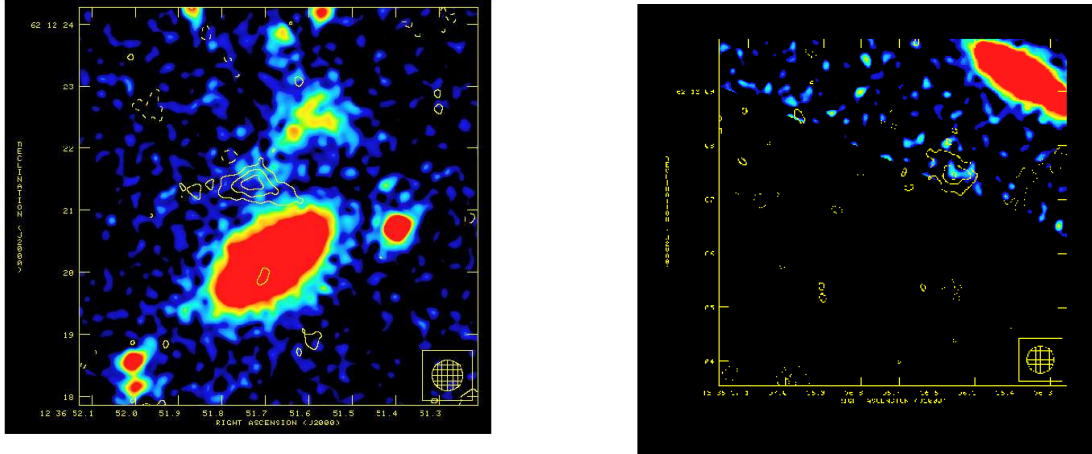


Figure 5. Left) Radio contours for VLA J123651+621221 are overlaid on the HDF-I image. The sub-mm source HDF850.1 lies $6''$ to the northeast. Right) VLA J123657+621206 is located at the very edge of the HDF but remains unidentified to $I = 28$. The source is heavily resolved by the MERLIN beam, but is firmly detected in the low resolution VLA data alone (Richards 1999b). SCUBA source HDF850.1 is located only $3''$ away, suggesting the two are the same object.

would have to be associated with particularly underluminous or dusty parent ellipticals. VLA J123642+621331 clearly does not fall into this category.

2. one sided radio jets: We cannot discount the possibility that some of our radio sources are the brightest jet of a nearby but displaced optical galaxy. In this case we would expect the parent galaxy to be a luminous elliptical with an AGN. We find no obvious candidates for this scenario.

3. very high- z AGN ($z > 6$) - Another possibility, is that some of the radio sources with very faint optical fluxes are at extreme redshifts, where the Lyman break blanks out the I continuum, placing them at $z > 6$. With our present radio sensitivity, we could have detected a nominal FR I galaxy to approximately $z = 10$. However, in several cases the radio emission is so resolved, it is unlikely to emanate from a compact AGN. On the other hand, at least two radio objects in the HDF remain unidentified to $H = 26$ (Dickinson, private communication) and $H = 28$ (Thompson et al. 1999).

4. high z -starbursts ($1 < z < 3$): Given that the majority of sub-millijansky radio sources are associated with star-forming galaxies, it is plausible that a tail of the parent galaxy population is so obscured by dust that only the radio emission is visible. In this case we would expect the radio emission to be steep spectrum (which it is in 18/19

of our objects) and the underlying galaxy to be a very red disk galaxy. Several of our objects best fit this description and we consider it the most plausible physical explanation.

We note that the surface density of these objects is about 0.1 square arcmin. There is likely some overlap with the faint sub-millimeter population, although at this point the numbers are too sparse to make any definitive statements. Further observations at near infrared and sub-millimeter wavelengths are necessary to discern the nature of the optically unidentified radio population.

5. Conclusions and Future Directions

We have shown that the microjansky radio population is associated primarily with star-forming galaxies. The clues that point to the radio emission being related to star-formation are 1) the steep radio spectra, 2) the small, but extended angular sizes of the sources, and 3) the identification with luminous disk galaxies. We have also isolated a population of optically faint radio sources ($I > 26 - 28$) which are possibly distant protogalaxies.

Radio observations provide a powerful tool in the study of star-formation to the earliest epochs. Together with deep near infrared and sub-mm observations, they have the potential to uncover all star-forming galaxies out to $z \sim 2$, free from dust extinction. The radio luminosity function of star-forming galaxies at moderate to high- z may ultimately reveal the global star-formation history, free from optical selection biases. The next generation of centimeter wavelength telescopes (the expanded VLA, Square Kilometer Array) will extend our knowledge of the radio properties of distant galaxies to redshifts of about 10. Figure 7 shows what the radio sky may look like at the nanojansky level.

I wish to thank the LOC for their generous financial support during the meeting. I thank my collaborators T. Muxlow, K. Kellermann, E. Fomalont, B. Partridge, R. Windhorst and I. Waddington.

References

- Aussel, H. et al. 1999, A& A, 342, 313
- Barger, A. et al. 1999, AJ, 117, 102
- Cohen, J. et al. 1996, ApJL, 471, 5
- Cram, L. E. 1998, ApJL, 506, 85
- Gallego, J., Zamorano, J., Aragon-Salamanca, A. & Rego, M. 1995, ApJL, 459, 43
- Helou, G., Soifer, B. T. & Rowan-Robinson, M. 1985, ApJL, 298, 7

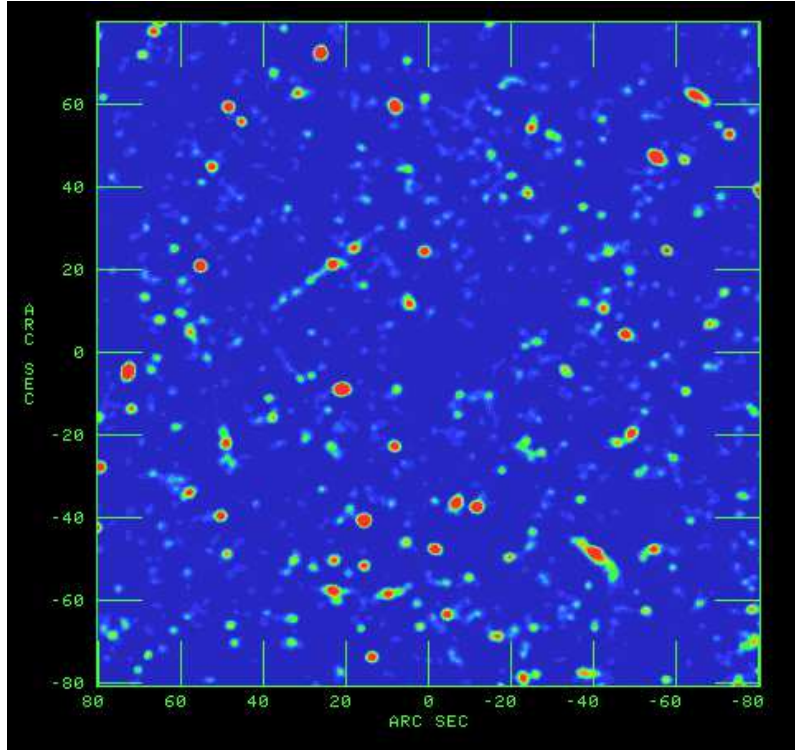


Figure 6. Shown is a simulation of a confusion limited HDF sized region at 1.4 GHz as seen by the proposed expanded VLA. The true field of view is 200 times larger, with a total of 40,000 detections above $0.5 \mu\text{Jy}$ (a factor of 80 deeper than the current VLA/HDF survey). Such observations could detect the Milky Way at $z = 1$ and Arp 220 up to $z = 10$ free from dust obscuration.

Hughes, D. et al. 1998, *Nature*, 393, 241
 Kronberg, P., Bierman, P. & Schwab, F. 1985, *ApJ*, 291, 693
 Muxlow, T. et al. 1994, *MNRAS*, 266, 455
 Muxlow, T. et al. 1999, in preparation
 Richards, E. A., submitted
 Richards, E. A. 1999b, *ApJL*, 513, 9
 Richards, E. A. et al. 1998, *AJ*, 116, 1039
 Rowan-Robinson, M. et al. 1993, *MNRAS*, 263, 123
 Smith, H., Lonsdale, C., Lonsdale, C. & Diamond, P. 1998, *ApJL*, 493, 17
 Soifer, B. T. et al. 1984, *ApJL*, 278, 7
 Soifer, B. T. et al. 1987, *ApJ*, 320, 238
 Thompson, R. et al. 1999, *AJ*, 117, 17
 Treyer, M., Ellis, R., Milliard, B., Donas, J. & Bridges, T. 1998, *MNRAS*, 300, 303
 Waddington, I., Windhorst, R. A., Cohen, S., Richards, E. A., Kellermann, K. I.,
 Fomalont, E. B. & Partridge, R. B. 1999, in preparation
 Williams, R. et al. 1996, *AJ*, 112, 1335